Spectral and angular-selective thermal emission from gallium-doped zinc oxide thin film structures

Enas Sakr*[a], Peter Bermel[a,b]
[a]School of Electrical and Computer Engineering, Purdue University, 465 Northwestern Ave., West Lafayette, IN, USA 47907-2035; [b]Birck Nanotechnology Center, 1205 W. State St., West Lafayette, IN USA 47907-2057

ABSTRACT

Simultaneously controlling both the spectral and angular emission of thermal photons can qualitatively change the nature of thermal radiation, and offers a great potential to improve a broad range of applications, including infrared light sources and thermophotovoltaic (TPV) conversion of waste heat to electricity. For TPV in particular, frequency-selective emission is necessary for spectral matching with a photovoltaic converter, while directional emission is needed to maximize the fraction of emission reaching the receiver at large separation distances. This can allow the photovoltaics to be moved outside vacuum encapsulation. In this work, we demonstrate both directionally and spectrally-selective thermal emission for p-polarization, using a combination of an epsilon-near-zero (ENZ) thin film backed by a metal reflector, a high contrast grating, and an omnidirectional mirror. Gallium-doped zinc oxide is selected as an ENZ material, with cross-over frequency in the near-infrared. The proposed structure relies on coupling guided modes (instead of plasmonic modes) to the ENZ thin film using the high contrast grating. The angular width is thus controlled by the choice of grating period. Other off-directional modes are then filtered out using the omnidirectional mirror, thus enhancing frequency selectivity. Our emitter design maintains both a high view factor and high frequency selectivity, leading to a factor of 8.85 enhancement over a typical blackbody emitter, through a combination of a 22.26% increase in view factor and a 6.88x enhancement in frequency selectivity. This calculation assumes a PV converter five widths away from the same width emitter in 2D at 1573 K.
Keywords: Epsilon-near-zero, Thermophotovoltaics, Thin films

1. INTRODUCTION

Highly spectral and angular-selective thermal emitters have recently been realized via nanostructuring of surface features; these structures may significantly benefit a range of applications, such as infrared light sources and thermophotovoltaics (TPV).[1–3] TPV is a method to convert heat into electricity via radiation of thermal photons toward a PV cell.[4] Typically, thermal photons are emitted by a hot radiator toward a PV cell to generate electricity. A good match between the emitted photon spectra and the PV bandgap is essential for enhancing TPV conversion efficiencies. Thus, there has already been a great deal of work to design spectrally-selective thermal emitters using both natural materials [5,6] and engineered photonic and plasmonic structures [7–10]. Nonetheless, much further improvement is possible if one also incorporates the angular selectivity, since this can greatly increase light reaching the cell, as quantified by the view factor [11]. Particularly, for planar compact TPV devices [12], this may relax the design parameters of the TPV device, by placing the emitter at larger separation distances, while maintaining a high view factor. Furthermore, with the need to place the entire set up inside a vacuum enclosure to reduce convection and conduction losses, effective cooling of the PV device becomes challenging. Directional thermal emission could allow for placing the PV device outside the vacuum enclosure, while allowing the device to cool through alternative methods like radiative cooling [13,14]. Consequently, a TPV system may benefit from a thermal emitter that simultaneously satisfy spectral and angular selectivity. In this work, we quantify the enhancement of the TPV efficiency expected when using a simultaneously spectral and angular selective thermal emitter.

*esakr@purdue.edu;

Physics, Simulation, and Photonic Engineering of Photovoltaic Devices VI, edited by Alexandre Freundlich, Laurent Lombez, Masakazu Sugiyama, Proc. of SPIE Vol. 10099, 100990A · © 2017 SPIE
CCC code: 0277-786X/17/$18 · doi: 10.1117/12.2251741

Several methods have been suggested to achieve simultaneous spectral and angular selective structures of thermal emitters, including plasmonic bandgap structures [15] with extremely narrow emission peaks, and plasmonic metasurfaces [2,16] with wider emission resonances and directional cones. For TPV applications, a sufficient spectral bandwidth as well as angular width are both necessary to maintain a practically-high open circuit voltage and view factor [17,18].

In this work, we present a novel method to simultaneously control spectral and angular properties of thermal radiation using epsilon-near-zero (ENZ) thin-films. ENZ materials provided a promising platform for different applications like electromagnetic tunneling, radiation pattern shaping, and manipulation of optical transmission [19–21]. Typically, this phenomenon emerges naturally in materials characterized by one or more strong resonances in their dispersion spectrum. Materials that exhibit this behavior (and their corresponding wavelength ranges) include polar dielectrics such as SiC and SiO_2 in the mid-IR regime [1,22], transparent conducting oxides in the near-IR regime [23], and metamaterial structures at tunable locations in the visible and infrared spectra [24]. Here, we predict that highly collimated spectral selective thermal emission can emerge from an engineered photonic structure that combines metamaterial perfect absorption phenomena in low-permittivity thin films with ENZ regime materials [25]. Gallium-doped Zinc Oxide (GZO) is employed as a low-permittivity material [23], backed by a metallic substrate, and topped by a high contrast grating (HCG) [26]. The HCG couples all modes above the light line to a guided mode in the low-permittivity film near the ENZ resonant wavelength. The perfect absorption phenomenon occurs in the wavelength regime where the permittivity of the thin film is larger than zero but less than one. A metallic substrate supports lateral propagation of waves in the low-permittivity film, leading to complete absorption in the thin film. Furthermore, we add an omnidirectional reflection mirror [27] on top to filter out non-directional modes associated with the ENZ dispersion [22,28]. Then, we utilize the suggested structure as a tailored thermal emitter for a TPV system, as shown in Fig. 1, to direct the spectrally-selective radiation towards an arbitrary distant PV cell. A view factor enhancement of 22.26% is demonstrated as well as an enhancement factor of 8.85x in the associated TPV efficiency.

In the following sections, the computational methods used to calculate the spectral and angular selectivity of the thermal emission, as well as the view factor enhancement and the TPV efficiency calculations are first presented. Then we discuss the physical phenomena that result in collimated spectrally-selective emissivity, followed by the obtained theoretical results.

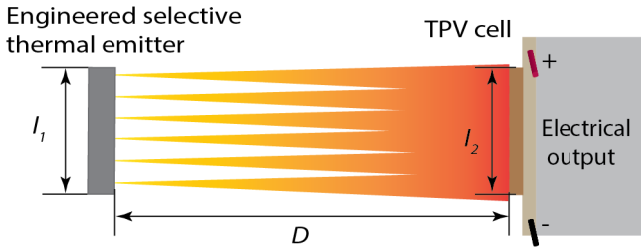

Figure 1. A TPV system with a selective thermal emitter exhibiting collimated, spectrally-selective emission onto a TPV cell. These combined features of the emitter maintain high conversion efficiencies, even for large emitter-cell separation distances *D*.

2. METHODOLGY

2.1 Emissivity computation

The emissivity dependence with wavelengths and emission angles is obtained by calculating absorptivity spectra, and then applying Kirchhoff's law of thermal radiation [29]. Kirchhoff's law states that, at thermal equilibrium, the emissivity equals the absorptivity for a given wavelength, incident angle and polarization. The p-polarized absorptivity as a function of wavelength and incident angle is given by $A(\lambda,\theta)=1-R(\lambda,\theta)-T(\lambda,\theta)$. Rigorous coupled wave analysis (RCWA) combined with an S-matrix algorithm is used to compute the emissivity of the emitter structure using a freely available software package, known as the Stanford Stratified Structure Solver (S^4) [30]. The dielectric function of the GZO thin film is obtained from the literature,[23] and fitted using a Lorentz-Drude model, which allows extrapolation to longer wavelengths. The emitter structure is assumed to be finite in one lateral dimension, and infinite in the other one.

2.2 View factor analysis

The view factor is defined as the proportion of the photons emitted from an area A_1 that reach a receiver of area A_2. It can be evaluated using the following general formula [11]:

$$F_{1-2} = \frac{1}{A_1}\int dA_1 \int dA_2 \frac{\cos\theta_1 \cos\theta_2}{\pi r^2}, \tag{1}$$

where θ_1 and θ_2 are the angles between the surface normal of the infinitesimal elements on the emitter and the receiver, respectively and the line connecting them, whose length is *r*. The integrand in (1) is then scaled by the wavelength- and angle-dependent emissivity function. A closed form expression of the view factor for a quasi-2D problem is calculated in previous work [18]. Thus, the wavelength dependent view factor can be computed as the ratio between the received normalized power at the PV cell $\phi_r(\lambda)$, and the total normalized emitted power in the upper hemisphere by the emitter $\phi_{em}(\lambda)$:

$$F_{1-2}(\lambda) = \frac{\phi_r(\lambda)}{\phi_{em}(\lambda)} = \frac{\int_{x_1=-l_1/2}^{l_{1/2}} dx_1 \int_{x_2=-l_2/2}^{l_2/2} dx_2 \left\{0.5\,D^2 \Big/ \left(D^2 + x_1^2 - 2x_1x_2 + x_2^2\right)^{3/2} \varepsilon(\lambda, x_1, x_2)\right\}}{\int_{x_1=-l_1/2}^{l_{1/2}} dx_1 \int_{x_2=-\infty}^{\infty} dx_2 \left\{0.5\,D^2 \Big/ \left(D^2 + x_1^2 - 2x_1x_2 + x_2^2\right)^{3/2} \varepsilon(\lambda, x_1, x_2)\right\}}, \tag{2}$$

where l_1, l_2, and D are the emitter's length, the receiver's length and the separation distance between them, respectively. The emissivity function $\varepsilon(\lambda, x_1, x_2)$ is extracted from the wavelength and angle-dependent emissivity $\varepsilon(\lambda, \theta)$ using the transformation $\tan\theta = (x_1 - x_2)/D$.

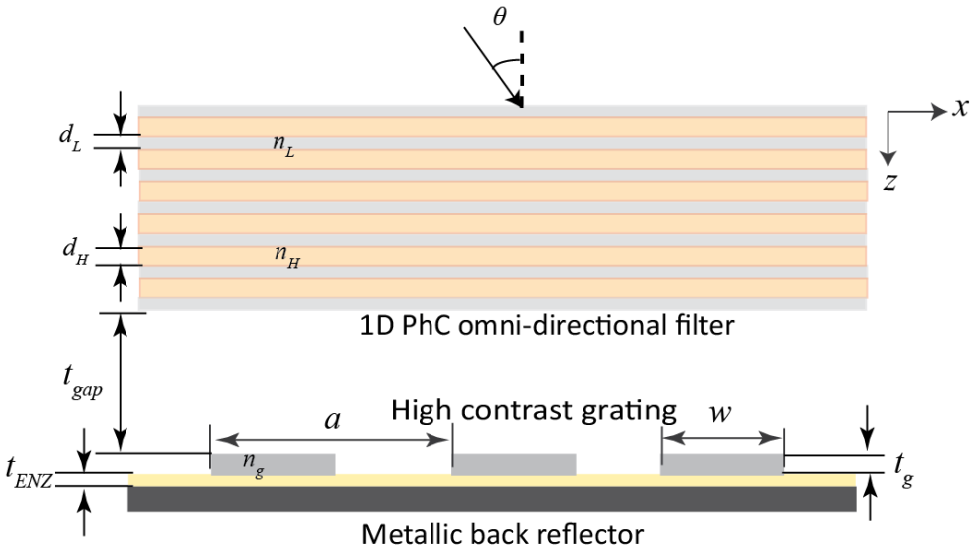

Figure 2. The proposed emitter structure. A thin ENZ layer of thickness t_{ENZ} on a metallic substrate is covered by a HCG to couple absorption modes in a cone around the normal direction near the positive ENZ wavelength regime. A 1D omni-directional mirror is placed above the structure to filter out the associated plasmonic absorption modes.

2.3 Application to TPV efficiency

The TPV system efficiency is given by the ratio of the output electric power to the total emitted power.[31] The corresponding formula reads $\eta = V_{OC} I_{SC} FF / P_{em}$, where V_{OC}, FF, I_{SC}, and P_{em} are the PV cell's open-circuit

voltage, fill factor, short-circuit current, and the total emitted power, respectively. The short-circuit current I_{SC} includes a wavelength-dependent view factor using $I_{SC} = \int_0^{\lambda_g} d\lambda J_{SC}(\lambda)\phi_r(\lambda)A_1$, where $J_{SC}(\lambda)$ is the photo-generated current at each wavelength and $\phi_r(\lambda)$ is the numerator of (2).

3. RESULTS

3.1 Emitter design

The emitter structure shown in Fig. 2, is composed of a GZO thin film as an ENZ material of thickness t_{ENZ} backed by a lossless metallic substrate of permittivity=-50. The ENZ thin film is covered by an HCG of thickness t_g=0.1a, where a is the period of the grating, and a groove width w=0.525a. For simplicity, we assume that the HCG is made of a lossless and dispersion-less material of refractive index n_g=3.5, similar to the refractive index of Si. Above this structure, a 1D PhC acting like an omni-directional mirror is placed at a vacuum gap of thickness t_{gap}=2.45a to filter out unwanted modes. The omni-directional mirror is composed of 18 bi-layers of alternating high- and low-index materials using the configuration $L^{0.5}(HL)^8H^{0.5}$. Here, we also assume lossless and dispersion-less refractive indices of 3.6 and 1.6 for the high- and low-index materials, respectively, and the ratio between their thicknesses is d_H/d_L=1/2. The ENZ layer's thickness is assumed to be 0.01a. In this analysis, only p-polarized incident modes in the Littrow mounting configuration [32] are taken into consideration.

3.2 Spectral and angular selective emissivity

From Kirchhoff's law of thermal radiation, it is possible to identify key emission modes from analyzing the absorption dependence at different wavelengths and incident angles. In absence of the top filter of the structure in Fig. 2, there are three types of modes that can be supported in the thin film ENZ. These modes are associated with the cross-over frequency of the GZO that can be readily controlled by adjusting the doping concentration and growth conditions [23]. When the ENZ layer is thin enough, it is possible to guide two perfect absorption modes [25]. The shift in the lateral momentum added by the HCG couples all the incident angles below the light line of the grating to high-k modes in the ENZ thin film. Per the diffraction equation of the grating, all incident angles less than a critical angle defined by $\theta_c = \sin^{-1}(1 - m\lambda/a)$, where λ is the wavelength, are coupled to guided modes that will be eventually absorbed in the ENZ layer. These modes appear particularly near the wavelengths where the permittivity of the ENZ thin film is larger than 0 but less than 1, and this in turn implies spectral selectivity. Consequently, the coupled modes are collimated, spectrally-selective absorption modes. However, the change of the dielectric constant at the cross-over frequency induces other types of modes, including the ENZ mode and the Ferrell-Berreman mode [22,24,28]. The ENZ mode is the long-range surface plasmon polariton mode that propagates near the surface of the thin film. Thus, the ENZ mode is a non-radiative mode that is efficiently coupled by the grating for angles larger than the critical angle θ_c. On the other hand, the Ferrell-Berreman mode is a radiative mode that is coupled to the ENZ thin film for p-polarization even in absence of the grating coupler. Thus, this mode is present for angles larger than θ_c. This mode is a result of volume-plasmon oscillations inside the thin film [33], and is noticeable for frequencies larger than the cross-over frequency. It is worth mentioning that the ENZ mode, the Ferrell-Berreman mode and the perfect absorption modes are all dependent on the film's thickness. For ultra-thin films, all the three types of modes are found close to the cross-over frequency, but they become well-separated for thicker films [22]. Also, the center frequencies and the quality factors of the perfect absorption modes both depend on the film's thickness [25]. Since the ENZ mode and the Ferrell-Berreman mode are non-directional near the cross-over frequency because of flat bands at large momentum values, there is a need to filter them out for the best performance. Thus, we use the omni-directional reflection mirror to keep only the perfect absorption modes, while recycling any other modes. In Fig. 3, contour plots of the calculated emissivity for the proposed emitter in Fig. 2 are shown as functions of the normalized frequency and the incident angle θ. Fig. 3(a) shows a frequency and angular selective mode at a frequency of 0.75c/a, and the half beam width at the normal direction is almost 12˚, as expected by the critical angle value. For longer wavelengths, the emissivity function is plotted in Fig. 3(b), where we only take into consideration the dispersion of the GZO layer. We notice a residual mode around a frequency of 0.4536c/a and an incident angle of ~70˚. This mode marks the unfiltered portion of the ENZ mode that is coupled by the HCG and

was present in absence of the filter at all incident angles around a frequency of 0.45*c/a* that is less than the cross-over frequency, located for this example at ~0.61*c/a*.

3.3 View factor and TPV efficiency enhancement

The TPV set up in Fig. 1 is used with the tailored TPV emitter described in Fig. 2. We assume both the emitter and the receiver are of the same lengths $l_1=l_2=l$, and separated by a distance $D=5l$. The PV cell is assumed to have a bandgap of 0.84 eV, a constant EQE of 1, and an ideality factor of 1. These conditions are close to an InGaAs PV cell, however, it is possible to shift the emission peak by changing the doping concentration, or by using Aluminum-doped Zinc-Oxide (AZO) [23] instead of GZO. For this computation, the period of the emitter structure *a* is taken to be 900 nm, and its temperature is 1573 K. We integrate over a wavelength range from 700 to 5000 nm to obtain the total TPV efficiency. The error associated with excluding the remainder of the emission spectrum should be less than 1% at the temperature range of 1573 K under consideration. At these operation conditions, we obtain a TPV efficiency of 5.31%, compared to a TPV efficiency of only 0.6% for a blackbody operating under the same conditions. Thus, the total enhancement of the TPV efficiency is approximately 8.85x compared to that obtained with a blackbody emitter. To quantify the efficiency enhancement contributed by frequency selectivity only, we turn off the angular selectivity, and compute the obtained efficiency in this case. The obtained TPV efficiency for an only frequency-selective structure is 4.13%, which is 6.88x larger than the TPV efficiency obtained if a blackbody emitter was used. This result demonstrates that angular selectivity alone increases TPV efficiency by 22.26%, compared to the spectrally selective baseline. This result is primarily driven by the significant enhancement of the view factor provided by the present structure considered.

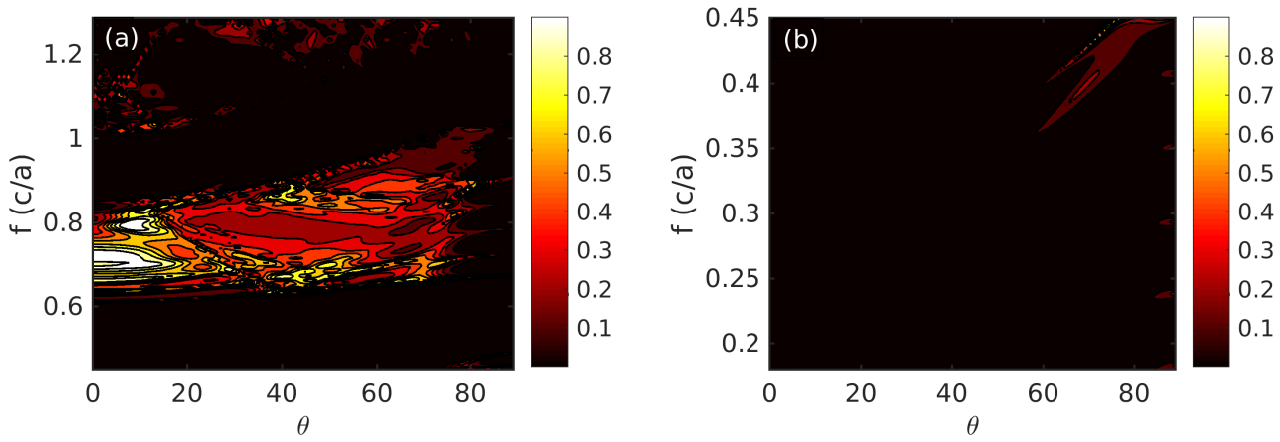

Figure 3. The p-polarized emissivity contour plots as functions of the normalized frequency *f* and the incident angle θ. (a) Emissivity contour plot for shorter wavelengths near the cross-over frequency (0.61*c/a*). A selective mode limited by $\theta_c = 12^\circ$ is noticeable. (b) Emissivity contour plot for lower frequencies. The unfiltered part of the ENZ mode where the dielectric function of the GZO becomes negative is still present at 0.45*c/a*.

4. DISCUSSION

Although the proposed structure maintains a high view factor for the perfect absorption modes, it still requires an omni-directional filter in proximity to the Metal-GZO-HCG structure to maintain high efficiencies via frequency selectivity. Accordingly, fabricating such a structure requires a reliable method to maintain a wavelength-scale vacuum-like gap in between. A possible implementation would utilize mechanical support spacers to maintain the structure at the required vacuum-gap separation [34,35]. Alternatively, an aerogel layer [36] can be filled in the vacuum-gap, as a highly transparent mechanical buffer layer. The latter approach could also facilitate the emergence of a non-trivial internal temperature gradient, since aerogels are known for their low thermal conductivity.

Also, the achieved results assume a high emitter temperature of 1573 K; this assumption however is limited by the melting point of the involved materials and the thermal stability of the structure at high temperatures. It is worth mentioning that the base ZnO material has a sufficiently high melting point. However, high doping levels could cause a significant drop in the melting point of the GZO film.

Another consideration of the design is the dielectric function change due to high temperature. Since transparent conducting oxides in general can be fitted with a Drude-Lorentz model, it is possible to tune the cross-over frequency as well as the damping coefficient to adjust for high temperature operations.[37,38] Taking an accurate high temperature model into consideration will help design appropriate thickness and geometric parameters of the HCG and the filter for fabrication. Parasitic losses in dielectrics and their high temperature dielectric functions should also be taken into consideration.

Finally, the polarization dependence of the HCG structure limits the application to the p-polarized component of the emitted heat. However, employing 2D structures [39] with symmetric shapes can also solve this problem by coupling s-polarized modes into the GZO thin film.

5. CONCLUSION

A spectrally and directionally-selective thermal emitter has been theoretically demonstrated using an ENZ thin film, a grating coupler, and a multilayer filter. A combination of the ENZ material properties and the perfect absorption phenomenon previously demonstrated in metamaterials is utilized to achieve both frequency and angular selectivity. An omnidirectional filter is used to filter out non-directional plasmonic modes and maintain high spectral selectivity. The proposed emitter structure shows a factor of 8.85x absolute enhancement of the TPV efficiency for a distant receiver compared to a blackbody emitter. The efficiency enhancement is a combination of frequency selective enhancement and angular selectivity to improve the view factor. In future work, adjustment of the doping concentration and modification of the grating design is necessary to match available technology of PV cells and to account for polarization effects, respectively.

ACKNOWLEDGMENTS

Support was provided by the NSF Award EEC 1454315 - CAREER: Thermophotonics for Efficient Harvesting of Waste Heat as Electricity, Northrop Grumman Aerospace Systems in support of "Ultra-thin metasurfaces for redirecting light and managing thermal emission," and the Department of Energy, under DOE Cooperative Agreement No. DEEE0004946 (PVMI Bay Area PV Consortium).

REFERENCES

[1] Greffet, J.-J., Carminati, R., Joulain, K., Mulet, J.-P., Mainguy, S.., Chen, Y., "Coherent emission of light by thermal sources.," Nature **416**(6876), 61–64, Macmillian Magazines Ltd. (2002).

[2] Blanchard, C., Lévesque, Q., Costantini, D., Jamois, C., Leclercq, J.-L., Coutrot, A.-L., Marquier, F., Milord, L., GRILLET, C., et al., "Directional and Selective Mid-Infrared Thermal Emitters for Sensing Applications," Adv. Photonics 2015, SeW2B.2, OSA, Washington, D.C. (2015).

[3] Sakr, E., Dhaka, S.., Bermel, P., "Asymmetric angular-selective thermal emission," Proc. SPIE 9743, Physics, Simulation, Photonic Eng. Photovolt. Devices V **9743**, 97431D (2016).

[4] Bauer, T., [Thermophotovoltaics: Basic Principles and Critical Aspects of System Design], Springer, Berlin (2011).

[5] Chubb, D. L., Pal, A. T., Patton, M. O.., Jenkins, P. P., "Rare earth doped high temperature ceramic selective emitters," J. Eur. Ceram. Soc. **19**, 2551–2562 (1999).

[6] Bitnar, B., Durisch, W.., Holzner, R., "Thermophotovoltaics on the move to applications," Appl. Energy **105**, 430–438 (2013).

[7] Rinnerbauer, V., Ndao, S., Yeng, Y. X., Chan, W. R., Senkevich, J. J., Joannopoulos, J. D., Soljačić, M.., Celanovic, I., "Recent developments in high-temperature photonic crystals for energy conversion," Energy Environ. Sci. **5**, 8815 (2012).

[8] Lenert, A., Bierman, D. M., Nam, Y., Chan, W. R., Celanović, I., Soljačić, M.., Wang, E. N., "A nanophotonic solar thermophotovoltaic device," Nat. Nanotechnol., 1–5 (2014).

[9] Wu, C., Neuner, B. I., John, J., Milder, A., Zollars, B., Savoy, S.., Shvets, G., "Metamaterial-based integrated plasmonic absorber/emitter for solar thermo-photovoltaic systems," J. Opt. **14**, 024005 (2012).
[10] Liu, J., Guler, U., Li, W., Kildishev, A., Boltasseva, A.., Shalaev, V. M., "High-temperature plasmonic thermal emitter for thermo-photovotaics," CLEO **1**, FM4C.5 (2014).
[11] Modest, M. F., [Radiative Heat Transfer], Academic Press (2013).
[12] Chan, W. R., Bermel, P., Pilawa-Podgurski, R. C. N., Marton, C. H., Jensen, K. F., Senkevich, J. J., Joannopoulos, J. D., Soljacic, M.., Celanovic, I., "Toward high-energy-density, high-efficiency, and moderate-temperature chip-scale thermophotovoltaics," Proc. Natl. Acad. Sci. **110**(14), 5309–5314 (2013).
[13] Raman, A. P., Anoma, M. A., Zhu, L., Rephaeli, E.., Fan, S., "Passive radiative cooling below ambient air temperature under direct sunlight," Nature **515**(7528), 540–544, Nature Publishing Group, a division of Macmillan Publishers Limited. All Rights Reserved. (2014).
[14] Zhou, Z., Sun, X.., Bermel, P., "Radiative cooling for thermophotovoltaic systems," Proc. SPIE 9973, Infrared Remote Sensing and Instrumentation XXIV, 997308 (2016).
[15] Biener, G., Dahan, N., Niv, A., Kleiner, V.., Hasman, E., "Highly coherent thermal emission obtained by plasmonic bandgap structures," Appl. Phys. Lett. **92**(8), 081913 (2008).
[16] Costantini, D., Lefebvre, A., Coutrot, A.-L., Moldovan-Doyen, I., Hugonin, J.-P., Boutami, S., Marquier, F., Benisty, H.., Greffet, J.-J., "Plasmonic Metasurface for Directional and Frequency-Selective Thermal Emission," Phys. Rev. Appl. **4**(1), 014023 (2015).
[17] Rephaeli, E.., Fan, S., "Absorber and emitter for solar thermophotovoltaic systems to achieve efficiency exceeding the Shockley-Queisser limit," Opt. Express **17**, 15145–15159 (2009).
[18] Sakr, E., Dimonte, D., Bermel, P., "Metasurfaces with Fano resonances for directionally selective thermal emission," MRS Adv. 1(49), 3307–3316 (2016).
[19] Mahmoud, A. M., Engheta, "Wave–matter interactions in epsilon-and-mu-near-zero structures," Nat. Commun. 5(5638), (2014).
[20] Luo, J., Xu, P., Gao, L., Lai, Y.., Chen, H., "Manipulate the Transmissions Using Index-Near-Zero or Epsilon-Near-Zero Metamaterials with Coated Defects," Plasmonics **7**(2), 353–358, Springer US (2012).
[21] Kim, J., Dutta, A., Naik, G. V., Giles, A. J., Bezares, F. J., Ellis, C. T., Tischler, J. G., Mahmoud, A. M., Caglayan, H., et al., "Role of epsilon-near-zero substrates in the optical response of plasmonic antennas," Optica **3**(3), 339 (2016).
[22] Vassant, S., Hugonin, J.-P., Marquier, F.., Greffet, J.-J., "Berreman mode and epsilon near zero mode," Opt. Express **20**(21), 23971 (2012).
[23] Naik, G. V., Kim, J.., Boltasseva, A., "Oxides and nitrides as alternative plasmonic materials in the optical range [Invited]," Opt. Mater. Express **1**(6), 1090 (2011).
[24] Newman, W. D., Cortes, C. L., Atkinson, J., Pramanik, S., DeCorby, R. G.., Jacob, Z., "Ferrell–Berreman Modes in Plasmonic Epsilon-near-Zero Media," ACS Photonics **2**(1), 2–7, American Chemical Society (2015).
[25] Luk, T. S., Campione, S., Kim, I., Feng, S., Jun, Y. C., Liu, S., Wright, J. B., Brener, I., Catrysse, P. B., et al., "Directional perfect absorption using deep subwavelength low-permittivity films," Phys. Rev. B **90**(8), 085411 (2014).
[26] Karagodsky, V., Sedgwick, F. G.., Chang-Hasnain, C. J., "Theoretical analysis of subwavelength high contrast grating reflectors.," Opt. Express **18**(16), 16973–16988 (2010).
[27] Winn, J. N., Fink, Y., Fan, S.., Joannopoulos, J. D., "Omnidirectional reflection from a one-dimensional photonic crystal," Opt. Lett. **23**, 1573–1575 (1998).
[28] Campione, S., Brener, I.., Marquier, F., "Theory of epsilon-near-zero modes in ultrathin films," Phys. Rev. B - Condens. Matter Mater. Phys. **91**(12), 1–5 (2015).
[29] Han, S. E., "Theory of thermal emission from periodic structures," Phys. Rev. B 80(15), 155108 (2009).
[30] Liu, V., Fan, S., "S4 : A free electromagnetic solver for layered periodic structures," Comput. Phys. Commun. 183(10), 2233-2244 (2012)
[31] Sakr, E. S., Zhou, Z.., Bermel, P., "High efficiency rare-earth emitter for thermophotovoltaic applications," Appl. Phys. Lett. **105**, 111107 (2014).
[32] Ko, Y. H., Niraula, M., Lee, K. J.., Magnusson, R., "Properties of wideband resonant reflectors under fully conical light incidence," Opt. Express **24**(5), 4542–4551 (2016).
[33] Kittel, C., [Introduction to solid state physics], Wiley (2005).
[34] Huang, M. C. Y., Cheng, K. B., Zhou, Y., Pesala, B., Chang-Hasnain, C. J.., Pisano, A. P., "Demonstration of piezoelectric actuated GaAs-based MEMS tunable VCSEL," IEEE Photonics Technol. Lett. **18**(10), 1197–1199 (2006).

[35] Tripathi, D. K., Jiang, F., Rafiei, R., Silva, K. K. M. B. D., Antoszewski, J., Martyniuk, M., Dell, J. M.., Faraone, L., “Suspended Large-Area MEMS-Based Optical Filters for Multispectral Shortwave Infrared Imaging Applications,” J. Microelectromechanical Syst. **24**(4), 1102–1110 (2015).
[36] Zhao, L., Yang, S., Bhatia, B., Strobach, E.., Wang, E. N., "Modeling silica aerogel optical performance by determining its radiative properties," AIP Adv. 6(2), (2016).
[37] Reddy, H., Guler, U., Kildishev, A. V., Boltasseva, A.., Shalaev, V. M., “Optical properties of gold thin films at elevated temperatures,” Opt. Mater. Express **6**(9), 5–6 (2016).
[38] Zhu, C., Li, J., Yang, Y., Lan, P., Huang, J., Lu, Y., Tan, R., Dai, N.., Song, W., “Tailoring the resonance wavelength and loss of highly Ga doped ZnO plasmonic materials by varied doping content and substrate temperature,” Thin Solid Films **605**, 95–101, Elsevier B.V. (2016).
[39] Sakat, E., Vincent, G., Ghenuche, P., Bardou, N., Dupuis, C., Collin, S., Pardo, F., Haïdar, R.., Pelouard, J.-L., “Free-standing guided-mode resonance band-pass filters: from 1D to 2D structures,” Opt. Express **20**(12), 13082 (2012).